JOURNAL OF PROPULSION AND POWER
Vol. 17, No. 4, July–August 2001

# Aeroacoustic Measurement of Transient Hot Nozzle Flows

Daniel R. Kirk,* Douglas O. Creviston,* and Ian A. Waitz†
*Massachusetts Institute of Technology, Cambridge, Massachusetts 02139*

**An assessment of a low-cost transient testing technique for obtaining acoustic measurements from hot, high-speed nozzle flows is presented. A shock tunnel was used to produce short-duration (10–20 ms) supersonic air jets from three sizes of American Society of Mechanical Engineers conic nozzles and a mixer-ejector nozzle typical of a high-speed civil transport (HSCT) aircraft application. A comparison between shock-tunnel transient noise data and steady-state data is presented. The assessment establishes the uncertainty bounds on sound pressure level measurements over the range of frequency bands, nozzle pressure and total temperature ratios, and nozzles scales for which the facility can be used as a substitute and/or complementary mode of investigation for steady-state hot-flow test facilities. Using the transient facility, far-field narrowband spectra were obtained at directivity angles from 65 to 145 deg, and the data were extrapolated to full-scale flight conditions. The constraint of short test duration is alleviated through the use of multiple runs to reduce the uncertainty associated with transient acoustic measurements. Sound pressure level vs frequency trends with nozzle pressure ratio and directivity angle are comparable between the steady-state and transient data for the conic and mixer-ejector nozzles. Conic nozzle results demonstrated that the transient noise data replicate the steady-state data to within ±2-3 dB, and the magnitude of effective perceived noise level values agree to within 1–3 dB depending on test condition and nozzle size. The mixer-ejector model demonstrated agreement with the steady-state noise data of around 2–5 dB on sound pressure level vs full-scale frequency over the range of nozzle pressure ratios and total temperature ratios relevant to the HSCT mixer-ejector development program. Trends in noise variation with azimuthal angle, as measured circumferentially about the inlet axis, as well as variation with mixer area ratio were also captured using transient testing.**

## Nomenclature

| | | |
|---|---|---|
| $A_{st}$ | = | shock-tube cross-sectional area |
| $A^*$ | = | nozzle throat area |
| $D_e$ | = | nozzle exit diameter |
| $l_{dn}$ | = | length of driven section |
| $l_{dr}$ | = | length of driver section |
| $l_{st}$ | = | length of shock tube |
| $P_{driven}/P_{atm}$ | = | driven/atmospheric pressure ratio |
| $P_{driver}/P_{driven}$ | = | driver/driven pressure ratio |
| $t_{exg}$ | = | exhaustion of test gas time limit |
| $t_{jet}$ | = | jet starting time |
| $t_{net}$ | = | total available test time |
| $t_{nozzle}$ | = | nozzle starting time |
| $t_{wave}$ | = | reflected wave test time limit |
| $\chi_{He}$ | = | helium mass fraction |
| $\Psi$ | = | directivity angle |

## I. Introduction

AIRCRAFT noise is currently one of the most significant environmental concerns facing air carriers.[1,2] Current projections of future demand for air transportation predict approximately 5% growth per year.[3] Furthermore, with an anticipated population density increase within the vicinity of airports, noise abatement is of increasing importance in the design of aircraft engines. Conventional steady-flow combustion or electric arc-heated facilities are currently employed as the primary means of acquiring fluid mechanic and acoustic data used to investigate noise suppressor nozzle concepts. Typical subscale nozzles cost between $10,000 and $100,000 and require several months to design and fabricate. Such time and fiscal constraints impose practical limits on the number of nozzle concepts and geometries that can be investigated and provide motivation for the development of more flexible and efficient testing techniques for the study of noise suppressor nozzles.

Received 22 September 1999; revision received 5 February 2001; accepted for publication 12 February 2001. 

*Graduate Student, Aero-Environmental Research Laboratory.
†Professor, Aeronautics and Astronautics, Aero-Environmental Research Laboratory.

One concept, the shock tube, is mechanically simple, has minimal operating and maintenance costs, and can generate flows with a wide range of total pressures and total temperatures comparable to steady-state facilities. Further, as a result of shock heating, the total temperature and pressure profiles at the nozzle inlet are uniform, eliminating the noise associated with entropy nonuniformities that are often present in steady-state, vitiated air facilities. The compromise made for mechanical simplicity and versatility is the brief duration of useful test time. Sufficient time must be allowed for the nozzle flow and free jet to reach a quasi-steady state before measurements can be made. However, if this constraint is met, the short run times become advantageous. The test nozzles are exposed to high-temperature flow for only a fraction of a second, thus relatively inexpensive stereo-lithography (SLA) nozzles ($2000–$5000 each), can be tested at realistic flow conditions. Conversely, nozzles for steady-state facilities are an order of magnitude more expensive because they must be robust enough to withstand pressures at elevated temperatures for extended periods of time.

The objective of the research described in this paper is to assess whether or not a shock-tunnel facility can be used to produce useful fluid mechanic and acoustic measurements of hot supersonic jets. It is shown, both analytically and experimentally, that the relevant fluid dynamic structures have sufficient time to reach a quasi-equilibrium state, that there is adequate test time to resolve the sound power spectrum levels, and therefore that useful far-field acoustic measurements can be acquired on scaled nozzles. Furthermore, a comparison between steady-state and transient shock tunnel data is presented.

The paper continues in Sec. II with a phenomenological overview of the operation of reflection-type shock tubes. Section III presents a facility overview and describes the test articles, apparatus, and data processing. Section IV contains a discussion of the testing methodology and procedures used in the experiment. Finally, Sec. V presents the results and a comparison with steady-state noise data for both the American Society of Mechanical Engineers (ASME) conic and mixer-ejector nozzles.

## II. Overview of the Use of Shock Tubes for Jet Testing

The fundamental purpose of the shock tube is to generate a reservoir of high temperature and high-pressure fluid that is expanded

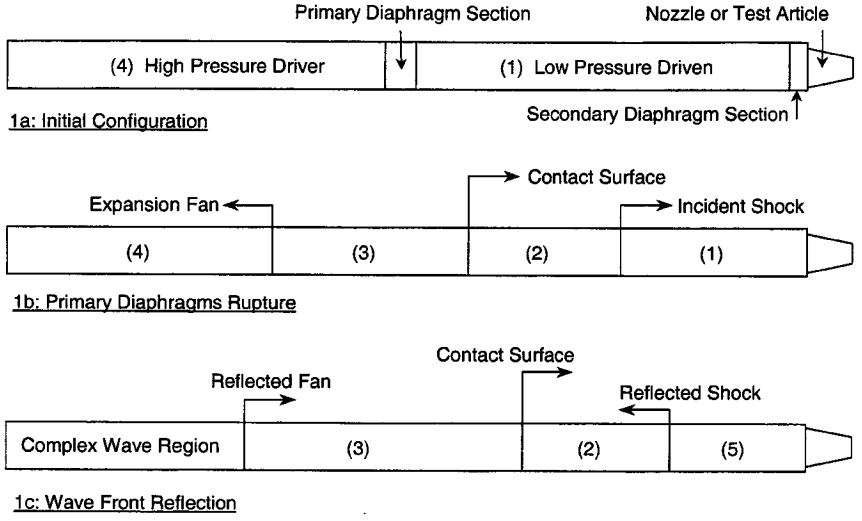


**Fig. 1 Shock-tube notation and wave phenomena.**

through a nozzle to create a hot supersonic jet. Initially, the tube is separated into a driven section, denoted as region (1), and driver section, denoted as region (4), by two thin primary diaphragms, as shown in Fig. 1a. The driven section contains the test gas, air for each test, and is typically evacuated to around one-fifth of an atmosphere. The driver section is evacuated and then filled with a mixture of helium and air to a pressure between 2 and 6 atm depending on the desired shock strength. A secondary diaphragm located between the driven section and the test article acts as a seal between the low-pressure air in region (1) and ambient air of the test chamber. The shock tube affords a great deal of flexibility because the driver pressure, gas composition, and the test gas pressure can be easily and accurately regulated to yield different stagnation temperatures and pressures behind the reflected shock.

When the section of the tube between the two primary diaphragms is evacuated, the pressure difference causes the diaphragms to press against knife blades and rupture. The driver gas acts like an impulsively started piston initiating a series of converging compression waves. The compression fronts rapidly coalesce into a shock wave, propagating through the driven section, accelerating, and heating the driven gas. Concurrently, a series of diverging expansion waves propagate through the driver gas mixture decreasing the pressure and accelerating the fluid in the direction of the nozzle. The state of the gas that is traversed by the incident shock wave is denoted by region (2) and that of the gas traversed by the expansion fan is denoted as region (3), as depicted in Fig. 1b. The interface, or contact surface, between regions (2) and (3) marks the boundary between the gases that were initially separated by the diaphragm. To first approximation, regions (2) and (3) can be assumed not to mix and are separated by the contact surface, which is analogous to the face of the piston. The test is initiated when the incident shock wave reaches the nozzle end of the tube, reflects from the end plate, and creates a region of stagnant, high-pressure, high-enthalpy fluid, denoted as region (5), which then ruptures the secondary diaphragm and expands through the nozzle to the desired conditions.

On either side of the contact surface, it is essential that the speeds of sound between regions (2) and (3) be identical to prevent extraneous waves from the reflected shock as it passes through the contact surface. These waves can substantially limit the available test time. To ensure that this does not occur, the speed of sound is matched by choosing the appropriate composition of gases for the driver section, using the matching condition:

$$\frac{\gamma_2}{a_2^2}\left[(\gamma_2+1)\frac{p_5}{p_2}+\gamma_2-1\right]=\frac{\gamma_3}{a_3^2}\left[(\gamma_3+1)\frac{p_5}{p_2}+\gamma_3-1\right] \quad (1)$$

If this condition is met, there will be no reflected disturbance.

The shock strength can be determined using the basic shock-tube equation, which relates the shock strength $p_2/p_1$ implicitly as a function of the known diaphragm pressure ratio $p_4/p_1$:

$$\frac{P_4}{P_1}=\frac{P_2}{P_1}\left[1-\frac{(\gamma_4-1)(a_1/a_4)(P_2/P_1-1)}{\sqrt{2\gamma_1}\sqrt{2\gamma_1+(\gamma_1+1)(P_2/P_1-1)}}\right]^{-2\gamma_4/(\gamma_4-1)} \quad (2)$$

Once the shock strength is determined, all other flow quantities can be determined from normal shock relations, and thus the thermodynamic and fluid mechanic properties of the jet are predicted. A detailed discussion of the gas dynamic model used to design the shock tunnel, as well as the effects of shock attenuation, freestream acceleration, shock-boundary-layer interaction, and imperfect reflections from an end plate are addressed in Refs. 4–8.

## III. Facility Description, Apparatus and Data-Processing Procedures

Section III describes the two facilities used in the assessment, the test articles, as well as a brief overview of the acoustic data-processing procedure.

### A. Transient Test Facility Description

The shock tube used in this experiment consists of a 7.3-m driven section and a 8.4-m driver, both constructed from 30-cm-diam stainless-steel pipe. A schematic of the shock tube used in this experiment is shown in Fig. 2, with many more details of the facility contained in Refs. 7 and 8. The tube is suspended on rollers to provide access to diaphragms and allow repositioning of the nozzles with respect to the microphones. The nozzles exhaust into an $8.3 \times 9.8 \times 3.7$ m anechoic test chamber treated with a 10-cm-thick fiberglass acoustic absorber, which results in 10–20 dB reduction in reflected acoustic intensity for frequencies above 500 Hz. This precaution is taken to avoid reflection of the jet noise during the test and to eliminate reverberations of the high-amplitude noise associated with the initiation of jet flow into the test chamber. The shock tunnel is equipped with a system that flushes the residual helium from the driver section after each test, ensuring that subsequent tests are not tainted by extraneous helium. Helium introduced into the test chamber after a test is removed via an exhaust fan.

### B. Test Articles

The sizes of ASME standard axismmetric nozzles used on the shock tube to assess facility performance are 5.1, 6.8, and 10.2 cm exit diameter. The conic nozzle used to acquire the steady-state data is 14.2 cm in exit diameter. More details, schematics, and pictures of the ASME nozzles can be found in Ref. 8. The mixer-ejector model

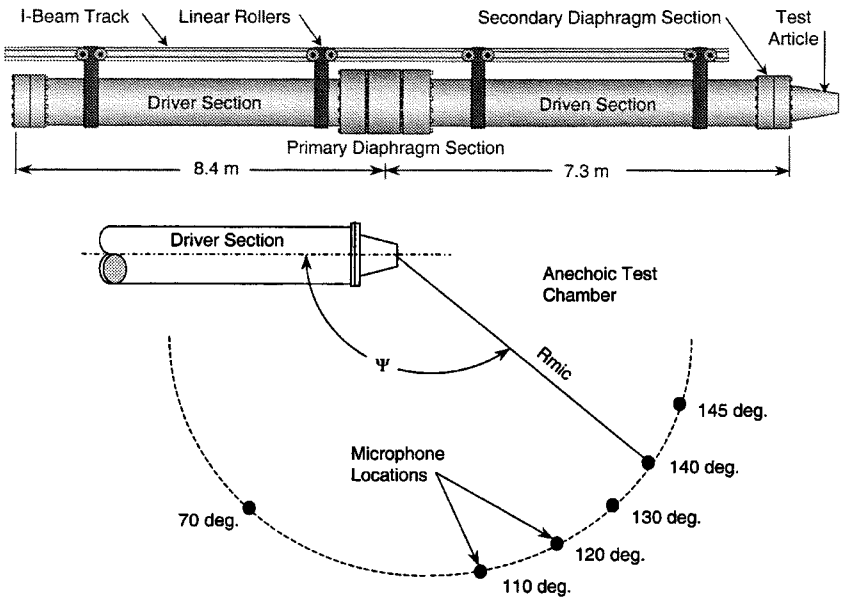


**Fig. 2 Shock-tube schematic and microphone location.**

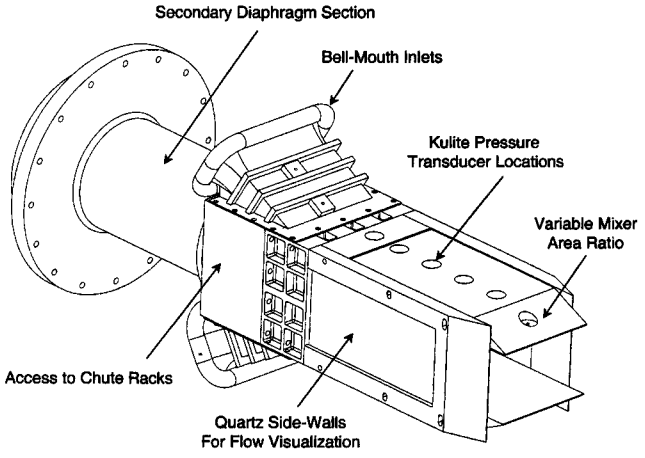


**Fig. 3 Mixer-ejector model schematic.**

tested at the facility is typical of a mixer-ejector nozzle that might be used in a high-speed civil transport (HSCT) application. An isometric view of the of the mixer-ejector nozzle used in the transient investigation is shown in Fig. 3. The chute racks tested in the model are made of either cast aluminum or plastic SLA. The aluminum chute rack was cast from a SLA model. The mixer-ejector model also features a compliment of 13 Kulite pressure transducers located along the centerline on both the top and bottom surfaces. The pressure measurements serve to confirm that the mixer-ejector model is operating at a quasi-steady mode by comparing with the pressure signatures acquired from the full-size steady-state model. The exact geometry of the device shown in Fig. 3, as well as the acoustic signatures and specific operating conditions of the device are proprietary.

### C. Acoustic and Fluid Mechanic Data Acquisition

Acoustic data were acquired using six Brüel & Kjær 4135 $\frac{1}{4}$-in. free-field microphones[9,10] positioned on a constant radius arc 3.7 m from the nozzle exit, as shown in Fig. 2b. The microphones were located at directivity angles comparable to the steady-state facility: 70, 110, 120, 130, 140, and 145 deg. Four Kulite XT-190 0-100 psia dynamic pressure transducers are flush mounted on the wall of the driven section of the shock tube. These four transducers are used to measure the primary nozzle pressure, shock speed, and test time (duration of the uniform pressure region). Using this instrumentation, the primary nozzle pressure ratio (NPR) can be determined with an uncertainty on the order of 0.5%. The total temperature ratio (TTR) is determined with an uncertainty on the order of 0.5% through measurement of the incident shock speed and use of the shock-tube equations. More information on the instrumentation and determination of NPR and TTR can be found in Refs. 8–11. Two computers are used to control the operation of the facility and acquire the pressure, noise, and thrust data. The control computer is configured with National Instrument's LabView and the required cards to control the sequence of 13 solenoid valves and 2 mass flow controllers necessary to fill and fire the facility, as well as to acquire and save the dynamic pressure data obtained from four wall-mounted pressure transducers in the shock tunnel. The second computer is configured with two ADTEK AD830 high-speed data acquisition boards, which enable it to simultaneously sample 16 channels at 12 bits, 330 Hz.

### D. Steady-State Test Facility Description

The steady-state data used for comparison were obtained from conic and mixer-ejector nozzles tested in the Boeing Low Speed Aeroacoustic Facility (LSAF). LSAF combines a large (20 m long × 23 m wide × 10 m high) anechoic test chamber with a 2.7 m × 3.7 m freejet wind tunnel. The steady-state acoustic data were obtained in $\frac{1}{3}$ octave bands over a frequency range from 200–8000 Hz, over a range of directivity angles from 52–146 deg. Acoustic instrumentation includes a traversing azimuthal microphone array at 4.6 m from the jet axis with additional free-standing microphones to augment the array measurement. Additional information on LSAF can be found on-line at http://www.boeing.com/assocproducts/techsvcs/boeingtech/bts_acoub.html.

### E. Acoustic Data Processing

The techniques that were used to reduce the data are typical of current industrial practice, and it was on this basis that we chose to make the comparison between the steady and transient data. The transient shock-tunnel acoustic data were processed using the NASA John H. Glenn Research Center Digital Acoustic Data System (DADS) as follows: the input was subdivided and converted into pressure vs time records, which were then processed to obtain spectra; the data were then processed to a 1-ft loss-less scenario taking into account instrument corrections and atmospheric attenuation; and then a fly-over transformation was performed. Frequency response characteristics and free-field corrections for microphone incidence angle were also incorporated into DADS. Steady-state sound pressure level (SPL) vs frequency data were also processed using DADS over the same frequency range as the transient data to ensure that the comparison presented was not influenced by processing scheme.

For an appropriate comparison to be made with steady-state results, the acquired data are compared at a full-scale diameter (101.6 cm for the conic nozzles) and over a simulated flight path

where the noise is flown over an observer at a distance of 496.5 m over a range of polar angles between 60 and 160 deg. Information beyond the range of polar angles measured is created by extrapolating the last angle's source spectrum to the new angle's propagation distance while taking into account atmospheric absorption. For the mixer-ejector model, which is not axisymmetric, azimuthal angle measurements are also made circumferentially 90 and 24 deg from the observer's ground location. Furthermore, each set of data is corrected to standard day ambient conditions. The extrapolation generates SPL vs frequency data for each of the polar angles, and the two data sets can be examined for agreement in magnitude of SPL over the full-scale frequency range, which depends on the size of the model nozzle. Overall sound pressure level (OASPL) and perceived noise level (PNL) at each polar angle are also calculated and compared to assess the directivity behavior of the transient and steady-state noise data.

## IV. Transient Test Time Limitations and Experimental Conditions

The principal constraint associated with using a shock tube for jet noise measurements is the short duration of the test time. Section IV.A contains a discussion of the limitations on test time and a comparison of analytical estimates to the values achieved with the transient facility. In Sec. IV.B the results of a statistical analysis are presented to determine the amount of test time needed to produce noise measurements with a given level of confidence. It will be shown that, in general, multiple runs of the shock tube are required.

### A. Determination of Useful Test Times and Comparison with Analytical Prediction

The time-distance history of the wave system within the shock tube is illustrated in Fig. 4. The duration of the steady flow through the nozzle is limited by either exhaustion of the test gas or the subsequent arrival of a reflected wave at the nozzle.

Time $t_1$ represents the duration of the test being limited by a reflection from the contact surface. As was discussed in Sec. II, this is eliminated by matching the speeds of sound in the gases to allow the reflected shock to pass undisturbed through the interface. Time $t_{wave}$ represents the duration of the test being limited by a secondary expansion (either the arrival of the reflected head of the primary expansion or the arrival of a weak secondary expansion generated if the reflected shock overtakes the tail primary expansion fan). The maximum test duration for a given geometry and temperature ratio occurs when the reflected shock simultaneously intersects the reflected head and tail of the expansion fan.

Achievable test times were predicted using methods described in Ref. 7. Table 1 presents a summary of the analytically predicted test

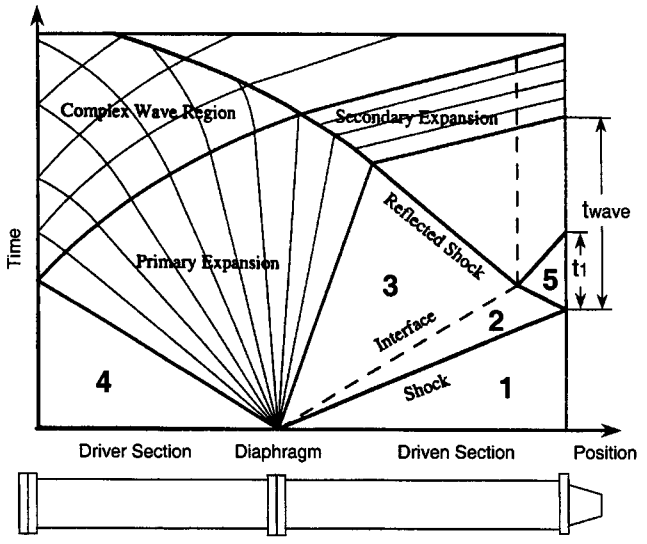


**Fig. 4 Time-distance history of the wave system in a shock tube.**

**Table 1 ASME nozzle analytically predicted test times (ms)**

| $D_e$ | NPR | TTR | $t_{wave}$ | $t_{exg}$ | $t_{nozzle}$ | $t_{jet}$ | $t_{net}$ | $t_{act}$ |
|---|---|---|---|---|---|---|---|---|
| 5.1 | 1.51 | 1.82 | 25.9 | 568 | 2.1 | 1.5 | 22.3 | 20 |
| 5.1 | 2.48 | 2.43 | 23.6 | 259 | 1.9 | 1.4 | 20.3 | 17 |
| 5.1 | 3.43 | 2.91 | 20.4 | 138 | 1.7 | 1.2 | 17.5 | 15 |
| 6.8 | 2.48 | 2.43 | 23.6 | 127 | 2.4 | 1.8 | 19.4 | 17 |
| 6.8 | 3.43 | 2.91 | 20.4 | 71 | 2.2 | 1.6 | 16.7 | 14 |
| 10.2 | 1.51 | 1.82 | 20.4 | 131 | 4.1 | 2.9 | 18.9 | 15 |
| 10.2 | 2.48 | 2.43 | 23.6 | 64 | 3.8 | 2.8 | 17.1 | 14 |
| 10.2 | 3.43 | 2.91 | 20.4 | 31 | 3.4 | 2.4 | 14.6 | 11 |

time $t_{net}$ and realized test time $t_{act}$ for eight combinations of ASME nozzle size and jet condition.

Provided the tailoring condition is met, the test time will be limited by the shorter of two time constraints: 1) the arrival of a reflected wave disturbance or 2) the exhaustion of the available test gas.

The wave impingement time at the nozzle $t_{wave}$ is a function of geometry $l_{dn}/l_{st}$ and TTR. The time to exhaust the test gas $t_{exg}$ is a function of TTR and the size of driven section and nozzle throat area. From each of these two time constraints, it is necessary to subtract the sum of the nozzle starting and jet development time to arrive at the net test time $t_{net}$. The nozzle starting time $t_{nozzle}$ is the time it takes to have started flow through the nozzle and is conservatively estimated as three nozzle flow-through times, varying with TTR. The jet starting time $t_{jet}$ is the time required for the turbulent jet to reach a quasi-steady state, which is a function of exit diameter, jet velocity, and potential core length. For each of the tests presented in Table 1, the net test time is not limited by the exhaustion of the test gas, but rather by a reflected wave disturbance.

Net test time decreases from approximately 23 to 15 ms with increasing nozzle scale and TTR and is not influenced by NPR. The last column of Table 1 shows the actual test time that was realized for the given test conditions. Useful test times are seen to be in consistent agreement with the analytically predicted values, with the actual values being slightly lower because of incident and reflected shock attenuation caused by viscous effects. A similar analysis was performed for the mixer-ejector nozzle using the pressure signatures from the Kulite pressure transducers to ascertain $t_{act}$. The comparison between the net predicted test time and the actual realized test time were in similar agreement as summarized for the ASME nozzles in Table 1, with typically 12–15 ms available for low NPR and TTR tests and 9–12 ms available for high NPR and TTR tests. The exact operating conditions of the mixer-ejector model cannot be given here, although the NPR and TTR range is similar to that shown in Table 1.

### B. Test Time Requirements for Statistical Confidence

The short duration of the net test time for the shock tube makes it important to understand how much total test time will be required to produce results that are in good agreement with steady-state facility data. It will be shown that shock tubes are most useful for simulating jet noise in relatively high-frequency bands since less time is required to accurately resolve the SPL in the relatively broader (in terms of Hz) $\frac{1}{3}$-octave bands.

To analytically predict the required test duration given a desired SPL confidence level, jet noise can be modeled as a chi-square random variable and statistically analyzed using the methods described by Hardin in Ref. 12. The analysis illustrates the principal trade between resolution and measurement uncertainty. As the bandwidth of the measured noise spectrum is reduced, the uncertainty in the estimate of the sound amplitude in each band increases. Figure 4 provides the results of the statistical analysis for a series of 12-ms test runs at 90% confidence from the 6.8 and 10.2-cm exit diameter nozzles at full-scale dB vs frequency. If multiple runs can be averaged together to increase effective test time, convergence around the steady-state data within the boundaries shown in Fig. 5 is expected. The convergence can be limited however, if systematic and run-to-run errors become significant. The figure shows that in order to obtain measurements of full-scale frequencies greater than 2 kHz

**Table 2 Summary of acquired data for ASME nozzles**

| | | Low | | | Mid | | | High | | |
|---|---|---|---|---|---|---|---|---|---|---|
| Test type | $D_e$ | NPR | TTR | Time | NPR | TTR | Time | NPR | TTR | Time |
| Steady-state | 14.2 | 1.51 | 1.82 | 1 s | 2.48 | 2.43 | 1 s | 3.43 | 2.91 | 1 s |
| Transient | 10.2 | 1.51 | 1.81 | 80 ms | 2.45 | 2.43 | 80 ms | 3.45 | 2.96 | 50 ms |
| Transient | 6.8 | N/A | N/A | N/A | 2.50 | 2.44 | 65 ms | 3.51 | 2.93 | 50 ms |
| Transient | 5.1 | 1.53 | 1.82 | 75 ms | 2.57 | 2.45 | 60 ms | 3.48 | 2.93 | 50 ms |

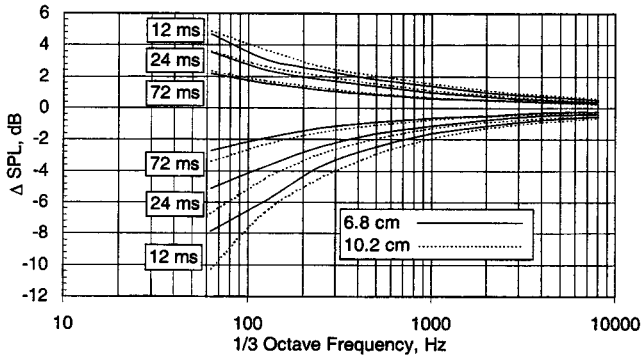


**Fig. 5 ΔdB resolution vs frequency for 90% confidence for 6.8- and 10.2-cm nozzles.**

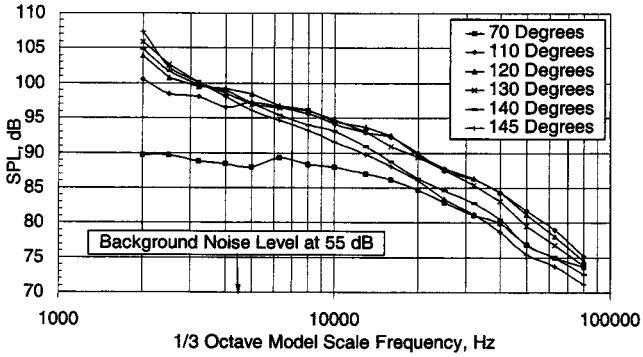


**Fig. 6 As-measured acoustic data, NPR = 1.51, TTR = 1.82, 5.1-cm nozzle.**

(30 kHz, 6.8 cm diam), which are within ±1 dB at 90% confidence, only one 12 ms test is needed. To resolve the spectra within ±1 dB at 90% confidence for frequencies greater than 500 Hz (7.4 kHz, 6.8 cm diameter), 72 ms of total test time (6-, 12-ms runs) is needed. More test time is needed as nozzle exit diameter increases to achieve the same level of confidence within a certain dB tolerance at a given full-scale frequency.

## V. Results and Discussion

A summary of the data used in the comparison between transient and steady-state jet noise is presented in Table 2 for the ASME conic nozzles. Three conditions, which are referred to as low (NPR = 1.51; TTR = 1.82), mid (NPR = 2.48; TTR = 2.43), and high (NPR = 3.43; TTR = 2.91) for convenience, were acquired with three ASME nozzle sizes in the transient investigation and with one nozzle size in the steady-state experiment. Table 2 also presents the nozzle pressure ratios and total temperature ratios achieved in the transient tests and the corresponding multiple run total test time.

The NPR and TTR of the transient tests were typically within 1% of the steady-state target values (which is within the data acquisition "drift" tolerances typically set by steady-state facilities), and the standard deviation of NPR with each run set (multiple runs at the same condition) was on the order of 0.05.

A sample of 18 ms of far-field acoustic data acquired from the 5.1-cm nozzle at the low condition is presented in Fig. 6. The plot shows SPL vs frequency for each of the six microphones, corresponding to directivity angles from 70 to 145 deg, located on a

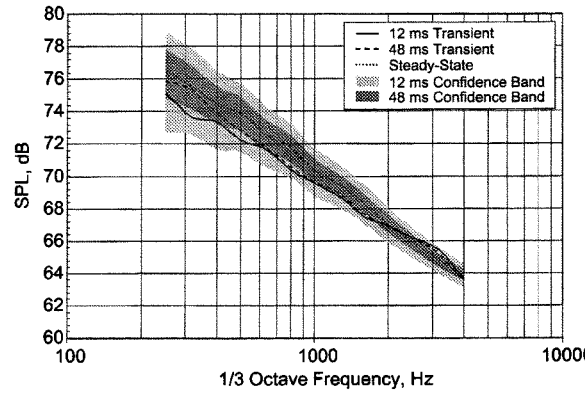


**Fig. 7 Use of multiple runs to decrease the uncertainty of transient acoustic data.**

constant radius arc 3.7 m from the nozzle exit. The data, which is acquired in narrowband, can then be extrapolated to any nozzle size, distance from the observer, or ambient condition, as was discussed in Sec. III.E. Figure 6 was plotted against $\frac{1}{3}$-octave frequencies for clarity. The plot shows several of the distinguishing characteristics typical of circular jet noise measured at constant radius. It can be seen that the aft directivity angles peak at a lower frequency and roll off faster in the high-frequency regime. Facility repeatability on a run-to-run and day-to-day basis was ascertained by examining the extrapolated data. Using the extrapolated data ensures changes in ambient conditions and associated atmospheric phenomena within the test chamber from test to test are properly taken into account. For each of the tests presented in Table 2, the run-to-run repeatability was found to be better than 0.5 dB for the conic ASME nozzles. On a series of tests on the same nozzle and set condition, the repeatability over the course of a six-week period was around 1 dB. Repeatability of the acoustic results from the mixer-ejector model was found to be around ±1 dB on a test-to-test and day-to-day basis.

### A. Use of Multiple Runs to Reduce Uncertainty of Transient Acoustic Measurements

Acoustic data from a series of runs at the same jet conditions were statistically analyzed to determine if data from multiple shots can be used to reduced the uncertainty associated with the measurements. Analysis of multiple runs generally shows a convergence analogous to the analytical prediction described in Sec. IV.B, with two to three shock tube shots typically required before convergence is achieved. Further convergence is limited by systematic errors. Figure 7 shows a comparison of the 120-deg directivity angle from the 5.1-cm nozzle at the low condition with 90% confidence intervals shown for the 12 and 48 ms of data as shaded bands. The plot is typical of each of the runs presented in Table 2 in that all angles and test conditions behaved in accordance with the analytically predicted confidence levels. The mixer-ejector data behaved in a similar fashion with the systematic errors associated with testing the device and a run-to-run repeatability of ±1 dB, in general, 2–3 shock-tube shots were required for convergence. Once again it is important to note that the convergence bands are applied in dB for $\frac{1}{3}$-octave frequencies.

### B. Transient vs Steady-State Comparison Methodology

The comparison between transient and steady-state data are made as SPL vs full-scale $\frac{1}{3}$-octave frequency to account for differences in

**Table 3 ASME nozzle performance comparison between transient and steady-state facilities**

| Nozzle, cm | NPR & TTR | Full-scale frequency range, Hz | Comparison with steady-state assessment: SPL vs full-scale frequency |
|---|---|---|---|
| 5.1 | Low | 250–4000 | ±2 dB on all directivity angles |
| 5.1 | Mid | 250–4000 | ±2 dB on 4 of 6 angles, ±3–4 dB on 120- and 130-deg angles |
| 5.1 | High | 250–4000 | ±2 dB on 5 of 6 angles, ±3 dB on 130-deg angle |
| 6.8 | Mid | 300–5300 | ±2–3 dB on all directivity angles |
| 6.8 | High | 300–5300 | ±2 dB on 5 of 6 angles, ±3 dB on 110-deg angle |
| 10.2 | Low | 500–6000 | ±2–3 dB on 3 of 6 angles, ±3–5 dB on 110-, 120-, and 130-deg angles |
| 10.2 | Mid | 500–6000 | ±2–3 dB on all directivity angles |
| 10.2 | High | 500–6000 | ±2–3 dB on all directivity angles |

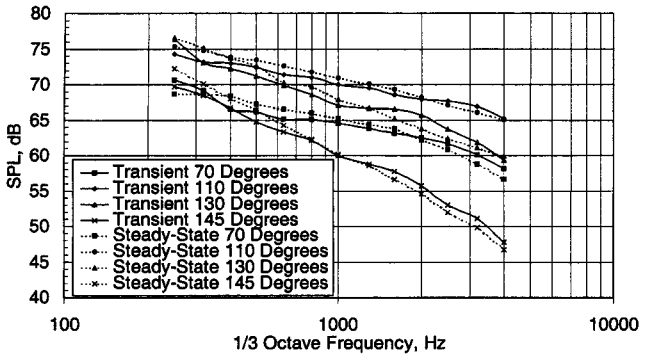


**Fig. 8 Extrapolated data comparison, NPR = 1.51, TTR = 1.82, 5.1-cm nozzle (transient) vs 14.2-cm nozzle (steady state).**

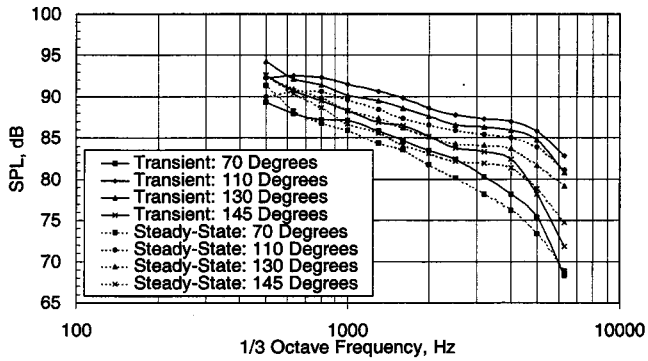


**Fig. 10 Extrapolated data comparison, NPR = 2.48, TTR = 2.43, 10.2-cm nozzle (transient) vs 14.2-cm nozzle (steady state).**

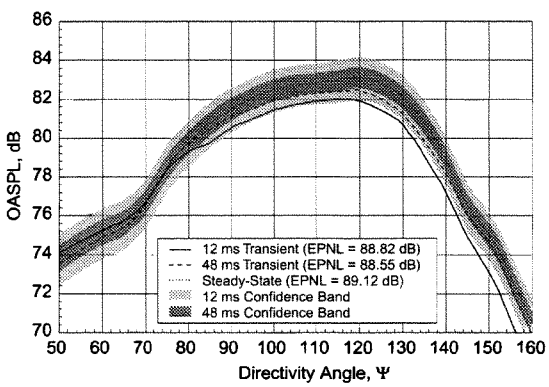


**Fig. 9 Extrapolated OASPL data comparison, NPR = 1.51, TTR = 1.82, 5.1-cm nozzle (transient) vs 14.2-cm nozzle (steady state).**

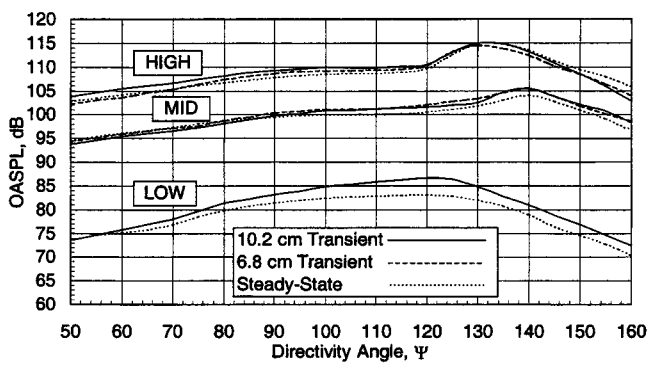


**Fig. 11 Extrapolated OASPL data comparison, 6.8-cm and 10.2-cm nozzles (transient) vs 14.2-cm nozzle (steady state).**

nozzle size, distance to microphones, atmospheric attenuation, and ambient conditions between the two test facilities. Additionally, the steady-state data were only available in $\frac{1}{3}$-octave frequency bands.

To ascertain how the jet noise generated from a transient shock-tube facility compares to steady-state noise data, a series of comparisons over the operating range shown in Table 2 were performed on the ASME and mixer-ejector model. Figure 8 shows a comparison of noise data from the 5.1-cm-diam nozzle (transient) and the 14.5-cm-diam nozzle (steady-state) at four directivity angles for the low condition, NPR = 1.51; TTR = 1.82. Once again both data sets were brought to a full-scale diameter of 101.6 cm, simulating the noise at 496.5 m from an observer when the source is directly overhead. The transient data consist of three shock-tunnel shots at the same condition combined back to back to give a total of 48 ms of test time. The four angles compared in the figure, one forward and three aft, are at 70, 100, 130 and 145 deg with a full-scale frequency range of comparison between 250–4000 Hz. The transient data exhibit agreement within 1–2 dB in magnitude over the entire frequency range. Directivity trends with position are also seen to be in agreement for all six angles. Note that the 120- and 140-deg angles have been omitted from this plot for clarity; however, these two angles also exhibit the same agreement with the steady-state noise data.

The corresponding static fly-over data for the 5.1-cm nozzle showing OASPL vs directivity angle are presented in Fig. 9 for test times of 12 and 48 ms. The figure shows a convergence of the transient data to the steady-state data as more test time is added. OASPL measurements from the 48 ms of transient data agree to within 1 dB in magnitude and show a comparable behavior with directivity angle with a peak in OASPL at around 120 deg. Confidence bands, derived from the time-series analysis described in Sec. IV.B and as shown in Fig. 7, for 12 and 48 ms of test time have been shown in Fig. 9. These confidence bands have also been processed through DADS, as described in Sec. III.E, for proper representation in Fig. 9. The transient data are seen to lie within the confidence interval.

### C. ASME Nozzle Noise Comparison

Another comparison between the steady-state and transient data is provided in Fig. 10 for the largest conic nozzle tested in the transient facility, 10.2-cm exit diameter. The figure shows a comparison of transient and steady-state SPL vs frequency at the mid-condition NPR = 2.48 and TTR = 2.43. The transient data contain a total of 52 ms of data from four shock-tube firings at the same jet conditions. The addition of more transient data did not show

a significant improvement in convergence to the steady-state noise signature. The agreement between the transient and steady-state data is around ±2 dB in magnitude between a full-scale frequency range of 500–6300 Hz. For frequencies lower than 500 Hz, limitations on jet development time become important. This possibility was taken into account when the full-scale low-frequency limit was set to 500 Hz for the 10.2-cm nozzle in Sec. III.D. The upper limit on the full-scale frequency is set by microphone frequency response.

Full-scale extrapolated data for all three conditions on the 10.2-cm and 6.8-cm nozzle are shown in Fig. 11. The high condition contains 46 and 54 ms of test time, and the midcondition contains 61 and 64 ms of test time for the 10.2- and 6.8-cm nozzles, respectively. The low condition was investigated for the 10.2-cm nozzle and contains 52 ms of transient data. The figure demonstrates that the transient data taken on 10.2- and 6.8-cm nozzles replicates the directivity pattern of the steady-state data at the high and midconditions with peaks at 130 and 140 deg, respectively. In contrast to the 5.1-cm nozzle, the 10.2-cm nozzle deviates by approximately 3–4 dB on the low condition at the 110- and 120-deg directivity angles, while the other angles show better agreement. The overall appearance of the OASPL vs directivity angle plot exhibits the same general shape and peak noise at around 120 deg. The achieved NPR of 1.52 for the 10.2-cm nozzle at the low condition was also slightly higher than the desired values of 1.51.

Although only a few plots comparing transient with steady-state data were presented in the preceding section, the results are representative of all of the conditions and nozzles scales tested. Table 3 presents a summary of the test conditions described in Table 2 and an assessment of the agreement between the transient and steady-state noise data.

Each of the ASME nozzles transient tests exhibited the same overall trends in magnitude and directivity as the steady-state data. The 5.1-cm nozzle exhibited better than ±2 dB agreement on each condition except for the 120- and 130-deg angles on the mid and high cases, which deviated by around 3 dB. The 6.8-cm nozzle agreed to within ±2 dB on the mid and high cases and to within ±3 dB on the 110-deg angle on the high case. Finally, the 10.2-cm nozzle agreed to within ±2 dB on the mid and high cases and had the worst agreement of any conic nozzle at the low condition, deviating by 3–5 dB at 110, 120, and 130 deg. All transient tests showed agreement with the steady-state data trends to with OASPL and PNL vs directivity angle.

An additional metric used to quantify the performance of the steady-state and transient data is the effective perceived noise level (EPNL), which is an internationally recognized unit for describing the noise of aircraft operation. To ensure proper comparison, the EPNL values for both the steady-state and transient tests were computed using DADS over the same full-scale frequency range. Table 4 summarizes this parameter for the conditions and ASME nozzle scales investigated.

Transient nozzle-to-nozzle tests agreed within approximately 1 dB ENPL for the mid and high cases. Each of the nozzles exhibited a higher value of EPNL, by about 1–2 dB, than the steady-state data at the midcondition. Once again the 5.1-cm nozzle displayed the best agreement, with EPNL matched to within 0.5 dB for the low and high conditions and approximately 1 dB for the midcondition.

**Table 4 ASME nozzle EPNL summary (dB)**

| NPR | Steady 14.2 cm | Transient 10.2 cm | Transient 6.8 cm | Transient 5.1 cm |
|---|---|---|---|---|
| 1.51 | 89.1 | 92.5 | N/A | 88.6 |
| 2.48 | 111.1 | 112.9 | 113.8 | 112.4 |
| 3.43 | 118.3 | 119.6 | 118.9 | 118.8 |

### D. Mixer-Ejector Nozzle Noise Comparison

This section compares transient shock-tube noise data to steady-state data from a mixer-ejector type nozzle, which was also acquired in Boeing's LSAF. The mixer-ejector nozzle is not an axisymmetric nozzle, and so variations in azimuthal angle were also investigated. Additionally, variation with mixer-area ratio or MAR (ratio of exit to primary throat area) were also investigated at a high, mid, and low condition, with the low being the smallest area ratio. Two chute racks, a cast aluminum and a plastic stereo-lithography version, were studied to ascertain whether the cheaper and more rapidly fabricated SLA chute rack could be used as a less-expensive substitute and still provide acoustic results that are in good agreement with the transient cast aluminum chute rack data. Because the exact geometry of the model and the acoustic results are proprietary, no plots similar to those shown in Figs. 5–11 can be shown. Comparisons, using the methodology outlined in Sec. V.B, were completed over a range of jet conditions somewhat similar to those shown in Table 2. In general, transient and steady-state data agree to within 2–5 dB on SPL vs full-scale frequency for all conditions using the cast aluminum chute rack. Table 5 summarizes the results of the mixer-ejector investigation over a full-scale frequency range of 250–4000 Hz.

The SLA chute rack was evaluated over a subset of the cases summarized in Table 4. In general the SLA chute rack was also within ±3–5 dB of the steady-state data. The SLA chute rack acoustic data agreed with the cast aluminum chute rack data (both data sets acquired using transient testing) to within ±1–2 dB for all conditions investigated.

For the mixer-ejector nozzle EPNL values were typically 2–4 EPNdB higher for the transient data as compared to the steady-state noise data. The trends in EPNL values between the low, mid, and high NPR condition showed agreement to about 1–2 EPNdB between the transient and steady-state data. Transient EPNL values were also in agreement with trends in MAR and azimuthal angle seen in the steady-state noise data. Mixer ejectors are complicated fluid mechanical devices that are very sensitive to small changes in geometry and operating condition. Differences in throat area, Reynolds number, lobe trailing-edge thickness and separation effects may play a role in the differences seen between the transient and steady-state

**Table 5 Mixer-ejector performance comparison between transient and steady-state facilities**

| NPR & TTR | MAR | Azimuthal angle, deg | Comparison with steady-state assessment 250–4000-Hz full-scale frequency range |
|---|---|---|---|
| Low | Low | 90 | ±2–4 dB on 100, 110, 120, 130 deg, ±3–5 dB on 70 deg |
| Low | High | 90 | ±2–5 dB on 100, 110, 120, 130 deg, ±3–5 dB on 70 deg |
| Mid | Low | 90 | ±2–4 dB on 120, 130 deg, ±3–5 dB on 70, 100, 110 deg |
| Mid | Mid | 90 | ±4–5 dB on 120, 130 deg, ±4–6 dB on 70, 100, 110 deg |
| Mid | High | 90 | ±2–3 dB on 120, 130 deg, ±3–5 dB on 70, 100, 110 deg |
| High | Low | 90 | ±1–2 dB on 70, 100, 110, 120 deg, ±2–3 dB on 130 deg |
| High | High | 90 | ±1–2 dB on all directivity angles |
| Low | Low | 24 | ±2–5 dB on 100, 110, 120 deg, ±3–5 dB on 70, 130 deg |
| Low | High | 24 | ±2–4 dB on 100, 110, 130 deg, ±3–4 dB on 70, 120 deg |
| Mid | Low | 24 | ±3–4 dB on 120, 130 deg, ±3–5 dB on 70, 100, 110 deg |
| Mid | Mid | 24 | ±3–5 dB on 120, 130 deg, ±4–6 dB on 70, 100, 110 deg |
| Mid | High | 24 | ±2–3 dB on 120, 130 deg, ±3–5 dB on 70, 100, 110 deg |
| High | Mid | 24 | ±1–2 dB on 70, 100, 110 deg, ±2–3 dB on 120, 130 deg |
| High | High | 24 | ±1–2 dB on 70, 100, 110, 120 deg, ±2–3 dB on 130 deg |

noise data. Specific conclusions from the mixer-ejector investigation include the following:

1) The SLA chute rack was robust enough to withstand even the highest nozzle pressures and demonstrated agreement with the cast aluminum chute rack to within 1–2 dB.

2) The transient data tend to drop off faster than the steady-state data at aft directivity angles, but on the whole are higher by about 2–3 dB than the steady-state noise data.

3) Variation with MAR was typically found to be on the order of 2 dB, whereas the steady-state data show variation of around 1 dB between the three cases studied.

4) Transient and steady-state data peaked at nearly the same directivity angle for all cases tested.

5) Variation in azimuthal angle for the transient data was in agreement with steady-state trends.

6) The use of multiple runs was found to reduce the uncertainty associated with making transient acoustic measurements with convergence being achieved after 2–3 shock-tube shots.

7) Run-to-run repeatability was on the order of 1 dB on a test-to-test basis.

## VI. Conclusions

A transient testing technique for the study of jet noise was investigated and assessed. A shock tube was used to generate a high-pressure and high-temperature air jet on which acoustic measurements were made on scaled nozzles. The short duration of the shock-tube experiments was statistically analyzed to determine how much test time is needed to produce results comparable to those of steady-state facilities. Transient tests were conducted on three sizes of ASME nozzles and a mixer-ejector typical of HSCT application and compared to results obtained from steady-state experiments at three NPR and TTR conditions. Full-scale SPL vs frequency plots demonstrated that the transient results exhibited agreement in magnitude and directivity trends with the steady-state data.

Specific conclusions from this investigation include the following:

1) A shock-tube transient testing facility can serve as a valuable tool for conducting jet noise research, with the cost of performing high-temperature jet noise experiments being reduced by more than an order of magnitude.

2) The use of multiple shock-tube shots at the same condition was shown to produce an acoustic signature that is comparable to that of steady-state facilities for both nozzle types. Run-to-run repeatability on the conditions was found to be within 1% on NPR and TTR and within 0.5 dB on SPL vs frequency for the ASME nozzles and 1.0 dB for the mixer-ejector nozzle.

3) The shock tunnel was shown to be an efficient facility for generating and acquiring noise data that are in agreement with steady-state data taken on comparably sized nozzles. For the ASME nozzles four out of eight conditions tested in this paper agreed to within $\pm 2$ dB of the steady state, and the remaining conditions showed deviation of 3–4 dB at one or two directivity angles. The mixer-ejector transient and steady-state data agree to within 2–5 dB on SPL vs full-scale frequency for all conditions tested.

4) The plastic stereo-lithography chute rack was shown to replicate the results of the cast aluminum variant to within $\pm 1$–2 dB for all transient tests conducted.

The shock tunnel was shown to be an efficient facility for generating and acquiring noise data that are in agreement with steady-state data taken on comparatively sized nozzles. Parametric testing can therefore be performed more economically and faster than in steady-state facilities, making transient shock-tunnel testing a valuable tool to serve as a complimentary mode of investigation for jet noise research.

## Acknowledgments

This work was supported Pratt & Whitney PO F760652 from NASA HSCT/CPC Prime Contract NAS3-27235. We thank E. Kawecki, B. Leland, K. Fouladi, and A. Stern for support and valuable technical advice throughout the course of the research. We also thank D. Forsyth and D. Arney of Boeing Company for facilitating this work and J. Bridges of NASA Lewis Research Center for setting up and providing continuous support for acoustic data processing and interpretation of the results. This material is based upon work supported under a National Science Foundation Graduate Fellowship.

## References

[1]*Environmental Review 1996*, International Air Transport Association, 1997, p. 97.

[2]Smith, J. T., *Aircraft Noise*, Cambridge Univ. Press, Cambridge, England, U.K., 1989, pp. 1–19.

[3]*Current Market Outlook 1996*, Boeing Aircraft Corp., Boeing Commercial Airplane Group, 1996, p. 1.

[4]Glass, I. I., and Patterson, G. N., "A Theoretical and Experimental Study of Shock-Tube Flows," *Journal of the Aeronautical Sciences*, Vol. 22, No. 2, 1955, pp. 73–100.

[5]Glass, I. I., "Theory and Performance of Simple Shock Tubes," Inst. of Aerophysics, Univ. of Toronto, UTIA Rept. 12, May 1958.

[6]Brabbs, A., and Belles, F. E., "Contact Surface Tailoring in Real Shock Tubes," *Proceedings of the 5th International Symposium on Shock Tubes and Shock Waves*, White Oak, Silver Spring, MD, 1965, p. 955.

[7]Kerwin, J. M., "Design of a Shock Tube for Jet Noise Research," Master's Thesis, Dept. of Aeronautics and Astronautics, Massachusetts Inst. of Technology, Cambridge, MA, June 1996.

[8]Kirk, D. R., "Aeroacoustic Measurement and Analysis of Transient Hot Supersonic Nozzle Flows," Master's Thesis, Dept. of Aeronautics and Astronautics, Massachusetts Inst. of Technology, Cambridge, MA, June 1999.

[9]Brüel and Kjær, "Instructions and Applications for Quarter Inch Condenser Microphones Type 4135/4136," July 1994.

[10]Brüel and Kjær, "Condenser Microphones and Microphone Preamplifiers for Acoustic Measurement," 1992.

[11]Allen, C. S., Vandra, K., and Soderman, P. T., "Microphone Corrections for Accurate In-Flow Acoustic Measurements at High Frequency."

[12]Hardin, J. C., "Introduction to Time Series Analysis," TR RP1145, NASA, March 1986.